Proton-to-alpha branching ratio in the ^{12}C+^{12}C fusion reaction at astrophysical energies*

Ruojun Yang (杨若君)[1] Ruiqi Chen (陈锐麒)[1] Xiao Fang (方晓)[1†] Yihua Fan (范翊华)[2,3]
Xiaodong Tang (唐晓东)[2,3‡] Yunju Li (李云居)[4§] Fengqiao Luo (罗枫桥)[5]

[1]Sino-French Institute of Nuclear Engineering and Technology, Sun Yat-sen University, Zhuhai 519082, China
[2]Institute of Modern Physics, Chinese Academy of Sciences, Lanzhou 730000, China
[3]School of Nuclear Science and Technology, University of Chinese Academy of Sciences, Beijing 100049, China
[4]China Institute of Atomic Energy, Beijing 102413, China
[5]University of Notre Dame, Notre Dame, IN 46556, USA

Abstract: The unique resonance features in the ^{12}C+^{12}C fusion reaction lead to significant fluctuations in the branching ratio $R_{p/\alpha}=\sigma_p/\sigma_\alpha$, making it difficult to determine $R_{p/\alpha}$ at astrophysical energies. By combining Hauser–Feshbach statistical-model calculations with constraints from direct charged-particle and gamma-ray measurements, we investigate the energy dependence of the averaged $R_{p/\alpha}$ and predict its behavior within the Gamow window. Owing to the strong energy dependence of $R_{p/\alpha}$, the corresponding reaction-rate ratios, $\langle\sigma v\rangle_p/\langle\sigma v\rangle_\alpha$, during core and shell carbon burning are determined to be 0.29, 0.45, and 0.52 at $T_9=0.5$, 1.0, and 1.2, respectively, which are significantly lower than the widely adopted CF88 constant value of 0.79. The implications of the revised $\langle\sigma v\rangle_p/\langle\sigma v\rangle_\alpha$ ratio for stellar nucleosynthesis and white-dwarf evolution are also discussed.

Keywords: carbon burning, Hauser-Feshbach, Talys, branching ratio, $R_{p/\alpha}=\sigma_p/\sigma_\alpha$

DOI: 10.1088/1674-1137/ae823a **CSTR:** 32044.14.ChinesePhysicsC.50094003

I. INTRODUCTION

The ^{12}C+^{12}C fusion reaction is a key process in stellar evolution, governing the carbon-burning phase in massive stars, the formation of white dwarfs, and the ignition of Type Ia supernovae and superbursts [1–4]. At astrophysical temperatures ($0.5\leqslant T_9\leqslant 1.2$), the reaction proceeds at sub-barrier energies corresponding to $E_{\rm cm}\sim 1-3$ MeV.

The fusion forms a highly excited ^{24}Mg compound nucleus with excitation energies of 15–17 MeV, which predominantly decays through the proton and α channels, ^{12}C(^{12}C,p)^{23}Na and ^{12}C(^{12}C,α)^{20}Ne. The branching ratio is

$$R_{p/\alpha}(E)=\frac{\sigma_p(E)}{\sigma_\alpha(E)}=\frac{S^*_p(E)}{S^*_\alpha(E)}, \tag{1}$$

where σ_p and σ_α are the fusion cross sections for the ^{12}C(^{12}C,p)^{23}Na and ^{12}C(^{12}C,α)^{20}Ne channels, respectively, and S^* is the modified astrophysical S-factor, which quantifies the competition between these two main reaction channels. S^* is defined as [5]

$$S^*(E_{\rm cm})=\sigma(E_{\rm cm})E_{\rm cm}\exp\left(\frac{87.21}{\sqrt{E_{\rm cm}}}+0.46E_{\rm cm}\right), \tag{2}$$

where $\sigma(E_{\rm cm})$ is the fusion cross section and $E_{\rm cm}$ is the center-of-mass energy in units of MeV. The modified S-factors for the ^{12}C(^{12}C,p)^{23}Na and ^{12}C(^{12}C,α)^{20}Ne channels are denoted by S^*_p and S^*_α, respectively.

This ratio has direct astrophysical implications. It governs the relative production of ^{23}Na and ^{20}Ne and influences nucleosynthesis pathways in massive stars [6]. It also serves as an important input for white dwarf models [2], particularly for interpreting stellar seismology observations.

The investigation of the proton-to-alpha branching ratio, $R_{p/\alpha}=\sigma_p/\sigma_\alpha$, is highly motivated by its distinct advantages over absolute cross-section measurements. Experimentally, extracting this ratio effectively cancels out major sources of systematic uncertainties, such as those originating from target thickness, beam current integra-

Received 17 May 2026; Accepted 24 June 2026; Accepted manuscript online 25 June 2026

* Supported by the GuangDong Basic and Applied Basic Research Foundation (2026A1515011317), National Natural Science Foundation of China (11875329, 12335009, U1632142), and National Key Research and Development program (MOST 2022YFA1602304)

† E-mail: fangx26@mail.sysu.edu.cn
‡ E-mail: xtang@impcas.ac.cn
§ E-mail: li_yunju@163.com

tion, and the absolute calibration of detection efficiencies. Consequently, $R_{p/\alpha}$ serves as an exceptionally clean and robust probe for exploring compound-nucleus decay dynamics.

Although numerous experiments on the $^{12}C+^{12}C$ fusion reaction have been performed over the past decades, significant discrepancies remain among the reported cross sections, particularly at low astrophysical energies. In Ref. [7], Li *et al.* employed the statistical-model code TALYS [8, 9] to estimate the branching ratios of unobserved (missing) channels in both the proton and α decay modes. By correcting the measured partial cross sections using these estimated branching ratios, they reconciled a substantial fraction of the discrepancies among the existing data sets. After applying these corrections, the experimental results agreed within approximately ±30% for $E_{\rm cm} \gtrsim 4$ MeV. The total fusion cross section was subsequently obtained by combining the proton, α, and neutron channels, and was compared with the proposed upper and lower limits.

In this work, we investigate the averaged behavior of the ratio $R_{p/\alpha}(E)$ by normalizing TALYS-based calculations from Ref. [7] to experimental cross sections corrected for missing channels. This approach enables us to derive an updated description of the competition between the $^{12}C(^{12}C,p)^{23}Na$ and $^{12}C(^{12}C,\alpha)^{20}Ne$ channels. We further perform an extrapolation to astrophysical energies and provide a revised evaluation of the corresponding reaction-rate ratio. The astrophysical implications are also discussed.

II. THEORETICAL FRAMEWORK

The decay is described using the Hauser-Feshbach statistical model [10]. For a reaction from an entrance channel α to an exit channel α', the averaged cross section can be expressed as [10]

$$\sigma_{\alpha\alpha'} = \pi\lambda\!\!\!^{-}{}_{\alpha}^{2} \times \sum_{J} \frac{2J+1}{(2I+1)(2i+1)} \frac{\left\{\sum\limits_{Sl} T_l(\alpha)\right\}^J \left\{\sum\limits_{S'l'} T_{l'}(\alpha')\right\}^J}{\left\{\sum\limits_{\alpha'',S''l''} T_{l''}(\alpha'')\right\}^J}, \tag{3}$$

where T_l denotes the optical-model transmission coefficient for a given partial wave.

A useful interpretation of Eq. (3) can be obtained in terms of decay branching ratios. For a given compound nucleus state with total angular momentum J, the probability that the system decays into a specific exit channel α' is determined by the ratio of its transmission coefficient to the sum of transmission coefficients for all energetically accessible channels. This defines the branching ratio.

$$b_{\alpha'}^{J} = \frac{\sum\limits_{S'l'} T_{l'}(\alpha')^J}{\sum\limits_{\alpha'',S''l''} T_{l''}(\alpha'')^J}, \tag{4}$$

where the denominator represents the total transmission strength over all open channels.

Note that the entrance channel consists of two identical ^{12}C bosons with $J^{\pi}=0^{+}$. Because the spatial wave function must be totally symmetric, only even partial waves ($L=0,2,4,\cdots$) are permitted in the entrance channel. This parity-dependent selection rule restricts the entrance-channel transmission coefficients T_l to even L and is rigorously included in our statistical calculations. The spin populations of the ^{24}Mg compound nucleus produced by $^{12}C+^{12}C$ fusion, calculated with the CCFULL code [11], are displayed in Fig. 4 of Ref. [7]. At sub-barrier energies, the spin-parity population of the ^{24}Mg compound nucleus is dominated by the 0^+, 2^+, 4^+, and 6^+ components. As the energy decreases, high-spin fusion channels are rapidly suppressed and become inaccessible. Over the stellar energy range $E_{\rm cm}=1-3$ MeV, the 2^+ state consistently accounts for approximately 56% of the total population, while the 0^+ fraction decreases monotonically from 39% at $E_{\rm cm}=1$ MeV to 33% at $E_{\rm cm}=3$ MeV.

The statistical model calculations were performed using the TALYS code, restricting the reaction mechanism to compound-nucleus formation and excluding pre-equilibrium and direct reaction contributions to maintain consistency with the low-energy physics of the $^{12}C+^{12}C$ system. The default global Optical Model Potential (OMP) was employed for both nucleons and α particles. The nuclear level density was calculated using the Constant Temperature Model matched to the Fermi Gas Model, and width fluctuation corrections were applied. The calculations were performed separately for each spin state; the final macroscopic results were constructed by weighting these discrete contributions according to the spin population predicted by CCFULL. Further computational details can be found in Ref. [7].

III. AVERAGED TREND OF THE $R_{p/\alpha}$ RATIO

Figure 1 presents a comprehensive comparison of the proton-to-alpha cross-section ratio for the $^{12}C+^{12}C$ fusion reaction obtained from different experimental approaches, including both direct and indirect measurements. All direct and indirect measurement data have been corrected for missing reaction channels following the prescription of Li *et al.* [7]. The pronounced resonance structures in the $^{12}C+^{12}C$ fusion reaction produce strong fluctuations in $R_{p/\alpha}$, making it difficult to determ-

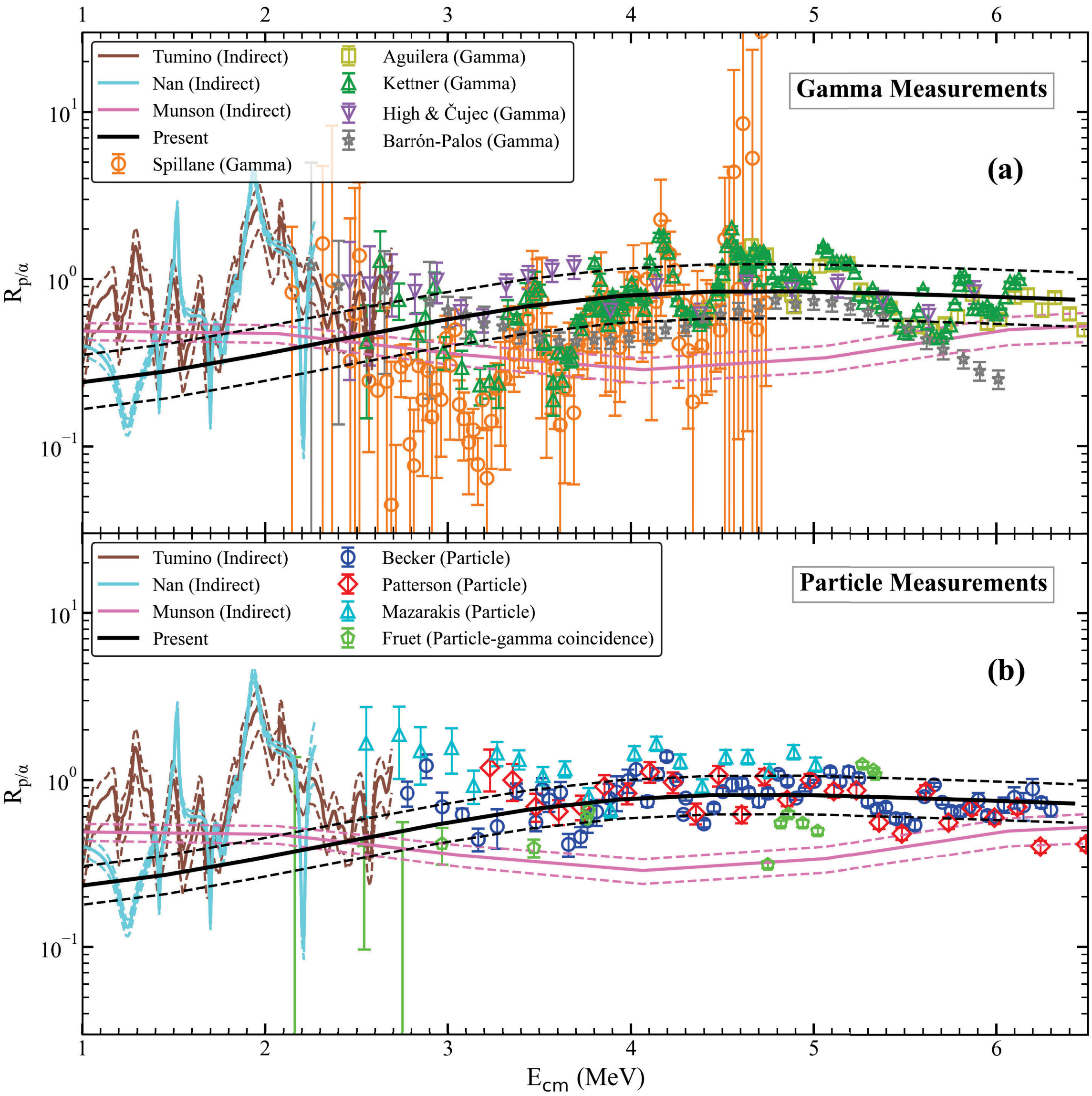

Fig. 1. (color online) The proton-to-alpha channel ratios are taken from direct measurements by Patterson *et al.* [5], Mazarakis and Stephens [12], High and Čujec [13], Kettner *et al.* [14, 15], Becker *et al.* [16], Aguilera *et al.* [17], Barrón-Palos *et al.* [18], Spillane *et al.* [19], and Fruet *et al.* [20], and from indirect methods by Munson *et al.* [21], Nan *et al.* [22], and Tumino *et al.* [23]. All measurement data were corrected for missing channels using the TALYS branching ratios from Li *et al.* [7]. The black solid and dashed lines in panels (a) and (b) represent the recommended mean and $\pm1\delta$ errors, respectively, based on our analysis of the gamma and particle datasets (fit parameters are listed in Table 1).

ine the ratio reliably at astrophysical energies.

Since the statistical model is expected to describe only the average behavior of the branching ratio, a purely theoretical prediction of the absolute proton-to-α cross-section ratio, $R_{p/\alpha}(E)$, remains challenging. This difficulty mainly arises from the presence of complex molecular resonances that are not fully incorporated in standard statistical-model calculations. To quantify the deviation between experimental data and statistical-model predictions, we define the ratio

$$R=\frac{(R_{p/\alpha}(E))_{\rm exp}}{f\times(R_{p/\alpha}(E))_{\rm Talys}}, \quad (5)$$

where $R_{p/\alpha}(E)_{\rm exp}$ and $R_{p/\alpha}(E)_{\rm Talys}$ represent the experimental ratios and the theoretical ratio predicted by TALYS, respectively, and f represents the scaling factor applied to adjust the TALYS calculations.

To incorporate the statistical uncertainties of individual data points, we employ a Monte Carlo resampling technique. For each experimental point, 1000 random samples are generated according to its Gaussian probability distribution, $N(\mu_i, \sigma_i^2)$. This parametric bootstrap approach naturally weights the dataset: high-precision measurements produce tightly clustered samples, whereas less precise data generate broader distributions. The resulting ensemble is fitted with a log-normal distribution. Note that the data are binned with equidistant intervals in logarithmic space ($\ln R$). Consequently, the Jacobian factor $1/R$ is intrinsically absorbed, and the distribution in this logarithmic space follows a standard Gaussian profile, which is fitted using

$$L(R) = A\exp\left[-\frac{(\ln R-\mu)^2}{2\delta^2}\right], \tag{6}$$

where A is a normalization constant, and μ and δ are the mean and standard deviation of $\ln R$, respectively. By varying the scaling factor f, the value of the ratio R (defined in Eq. (5)) can be adjusted. An appropriate choice of f allows us to normalize the experimental ratio $(R_{p/\alpha}(E))_{\rm exp}$ to the scaled TALYS theoretical prediction $f\times(R_{p/\alpha}(E))_{\rm Talys}$, shifting the central value of R to unity. Consequently, the mean of the logarithmic ratio becomes zero ($\ln 1 = 0$), corresponding to a central value $\mu\approx 0$ for the normal distribution of $\ln R$. For each dataset, f was systematically optimized such that μ converged to zero within a tolerance of ± 0.002. Using the standard deviation δ obtained from the log-normal fit of R, we define the 1δ confidence interval as $[e^{\mu-\delta}\approx e^{-\delta}, e^{\mu+\delta}\approx e^{\delta}]$. Therefore, the upper and lower limits of f are estimated as fe^{δ} and $fe^{-\delta}$, respectively.

The scaled ratio, $f\times R_{p/\alpha}(E)_{\rm Talys}$, is used to predict the ratio down to astrophysical energies, while the δ obtained from the fit is used to estimate the deviation between the true ratio and the TALYS prediction.

Different methods and measurements introduce different systematic uncertainties. In the following sections, we group the evaluations of $R_{p/\alpha}(E)_{\rm exp}$ into three categories: measurements with charged-particle spectroscopy, measurements with γ-ray spectroscopy, and indirect measurements. The f and $\pm\delta$ values obtained for each category are compared. Based on this comparison, we recommend the best value of f together with the corresponding uncertainty δ (*i.e.*, $\pm\delta$).

A. Fit to charged particle data

As shown in Fig. 11 of Ref. [24], at higher energies (4.0 MeV $< E_{\rm cm} <$ 6.0 MeV), direct charged-particle measurements [5, 12, 16] are generally consistent. However, below ~ 4 MeV, the proton- and α-channel S^* values reported by Patterson and Mazarakis remain systematically higher than those of Becker. If these discrepancies stem from systematic uncertainties—such as those associated with target thickness, beam-current integration, and the absolute calibration of detection efficiencies—the experimental $R_{p/\alpha}$ ratio can largely cancel these uncertainties.

We excluded the data of Mazarakis [12] from our analysis due to a well-documented systematic energy offset of approximately 100 keV [17] and suspected beam-induced background from deuterium contaminants at low energies.

To establish a robust experimental trend for the proton-to-alpha branching ratio $R_{p/\alpha}$, we performed a statistical comparison between the TALYS prediction and the direct charged-particle data. As detailed in Table 1, our primary analysis focuses on the energy window $E_{\rm cm} = 3.5-6.4$ MeV. This interval is specifically chosen to avoid the deep sub-Coulomb regime ($E_{\rm cm} < 3.5$ MeV), where a degraded signal-to-noise ratio and significant background interference would otherwise introduce disproportionate influence and potential bias into the statistical inference.

The average ratio $R_{p/\alpha}$ was extracted using a Log-Normal distribution defined by Eq. (6). Because the experimental uncertainties in cross-section ratios are predominantly multiplicative and the observables are strictly non-negative, the Log-Normal distribution provides a more rigorous statistical representation than a conventional Gaussian distribution.

The results of this fitting procedure are comprehensively illustrated in Fig. 2. Panel (b) of Fig. 2 shows the ratio of the experimental data to the scaled TALYS prediction, and panel (c) displays the corresponding Log-Normal distribution of these ratios. By fitting the data sets of Becker and Patterson within $E_{\rm cm} = 3.5-6.4$ MeV, we obtained an optimal scaling factor of $f = 0.690$. The statistical analysis yielded a logarithmic standard deviation of $\delta = 0.265$. Consequently, the 1δ uncertainty band is defined by multiplicative factors $e^{-\delta} = 0.767$ (lower limit) and $e^{+\delta} = 1.303$ (upper limit).

The scaled TALYS prediction, together with this precisely defined uncertainty band, is plotted against the experimental data in Fig. 2(a), demonstrating excellent overall agreement within the selected energy window. Furthermore, Table 1 summarizes these fit parameters alongside those derived from other measurement techniques (γ-ray and indirect measurements), demonstrating that the direct charged-particle data provide a tightly constrained average trend for calibrating the theoretical $R_{p/\alpha}$ ratio.

Note that extracting the total cross sections from experimental data requires correcting for unobserved weak decay channels (*e.g.*, highly excited states), for which we used the statistical model estimates from Li *et al.* [7]. While this introduces some model dependence into the "experimental" ratio, these unobserved channels typically account for a small fraction of the total reaction yield. Consequently, the extracted central scaling factor f remains primarily constrained by the direct measure-

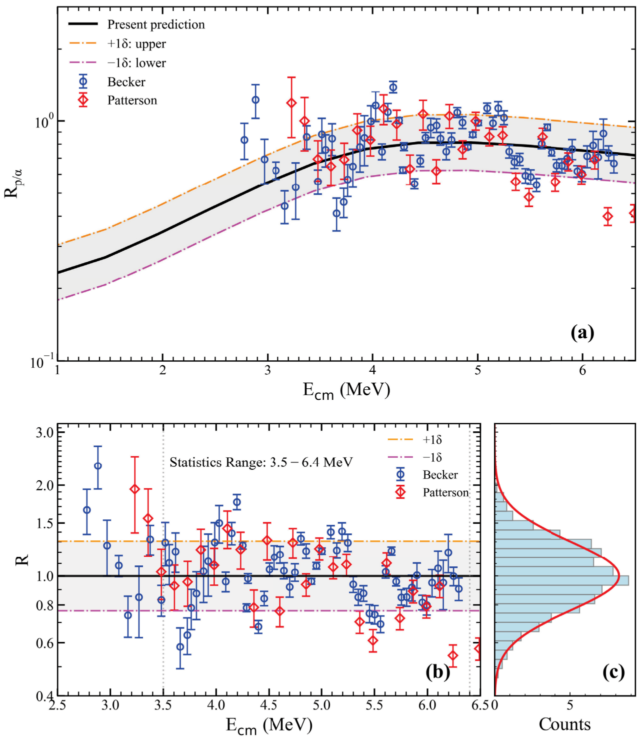

Fig. 2. (color online) (a) Experimental ratio $R_{p/\alpha}$ compared with the present prediction and its $\pm1\delta$ uncertainty band. The central line corresponds to a scaling factor of 0.690, with lower and upper uncertainty bounds of 0.767 and 1.303, respectively. Experimental data from Patterson *et al.* and Becker *et al.* are shown for comparison. (b) Ratio of experimental data to the scaled TALYS prediction, illustrating the extraction of the normalization factor. (c) Distribution of the ratio values shown in panel (b), together with a Log-Normal fit.

ments of the dominant decay branches.

B. Fit to γ-ray spectroscopy data and global analysis

In addition to charged-particle measurements, γ-ray spectroscopy provides an alternative method for extracting partial cross sections. As shown in Fig. 1, the ratios derived from γ-ray data exhibit significantly larger fluctuations, with $R_{p/\alpha}$ varying widely from approximately 0.2 to 2.0, whereas the ratios extracted from charged-particle measurements fluctuate within a narrower range (approximately 0.5 to 1.5). γ-ray spectroscopy detects fewer reaction channels than charged-particle measurements. Consequently, the extracted ratios are more sensitive to the complex cluster structures and molecular resonances of the $^{12}C+^{12}C$ system near and below the Coulomb barrier, resulting in significantly larger fluctuations.

We applied the Log-Normal distribution defined in Eq. (6) to fit the TALYS prediction to the datasets of Aguilera *et al.* [17], Kettner *et al.* [14, 15], and High and Čujec [13]. As summarized in Table 1 and depicted in Fig. 3, fitting these datasets over the reliable energy range $E_{cm} = 3.7-6.4$ MeV yields an optimal scaling factor of $f = 0.715$. The statistical analysis of the data-to-theory ratios yields a logarithmic standard deviation, corresponding to multiplicative uncertainty bounds of $e^{-\delta} = 0.689$ (lower limit) and $e^{+\delta} = 1.452$ (upper limit). Remarkably, this central scaling factor ($f = 0.715$) is in excellent agreement with the factor independently derived from charged-particle data ($f = 0.690$). The noticeably wider uncertainty band, however, correctly captures the large intrinsic resonance fluctuations present in the γ-ray channels.

Given the excellent systematic agreement in the central scaling factors derived independently from the primary charged-particle and γ-ray datasets, we construct a comprehensive global fit to establish the final theoretical trend. By combining the data from Patterson, Becker, Aguilera, Kettner, and High and Čujec in the energy range $E_{cm} = 3.5-6.4$ MeV, we obtain a global optimal scaling factor of $f =$ 0.698, which is the recommended value from this work, with an uncertainty band corresponding to the multiplicative factors $e^{-\delta} = 0.708$ and $e^{+\delta} = 1.412$ (see Table 1 and Fig. 4). This combined fit confirms the normalization of the TALYS calculation, demonstrating that the ratio $R_{p/\alpha}$ converges to a consistent value regardless of the distinct systematic errors inherent to particle or γ-ray detection techniques. At sub-barrier energies, a value of $f \approx 0.7$ suggests that the standard OMP may underestimate the α-particle penetrability for the $^{12}C+^{12}C$ system.

Table 1. Log-normal fit results for experimental $R_{p/\alpha}$ ratios normalized to the present prediction.

No.	Fit dataset	Fit range	f	δ	$e^{-\delta}$(lower)	$e^{+\delta}$(upper)
1	Particle: Becker [16], Patterson [5]	3.5-6.4 MeV	0.690	0.265	0.767	1.303
2	Gamma: Aguilera [17], Kettner [14, 15], High and Čujec [13]	3.7-6.4 MeV	0.715	0.373	0.689	1.452
3	Particle & Gamma: Becker [16], Patterson [5], Aguilera [17], Kettner [14, 15], High and Čujec [13]	3.5-6.4 MeV	0.698§	0.345	0.708	1.412
		3.7-6.4 MeV	0.698	0.330	0.719	1.391
4	Indirect: Nan [22]	1.0-3.0 MeV	1.319	0.773	0.462	2.166
5	Indirect: Nan [22], Tumino [23]	1.0-3.0 MeV	1.443	0.698	0.498	2.010

§ Recommended value 0.698 for scaling factor *f*.

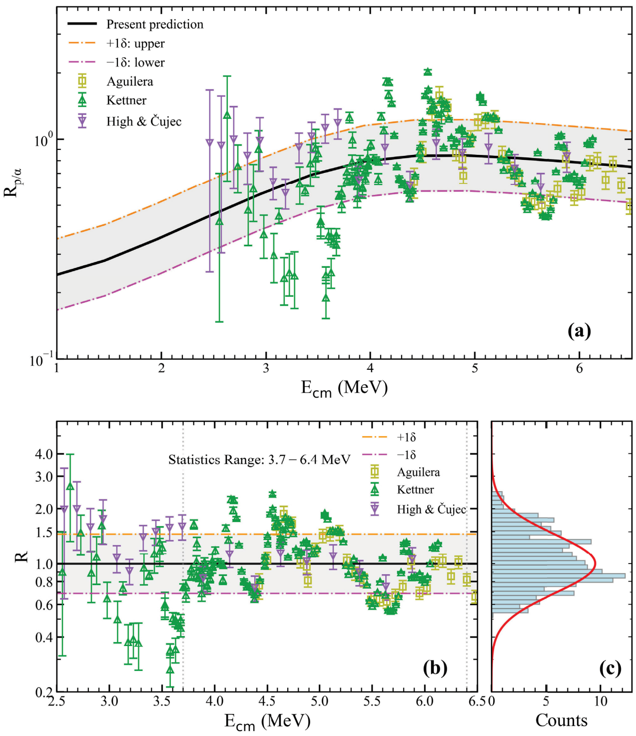

Fig. 3. (color online) (a) Experimental ratio $R_{p/\alpha}$ compared with the present prediction and its $\pm 1\delta$ uncertainty band. The data are from Aguilera, Kettner, High, and Čujec. (b) Ratio of experimental data to the TALYS calculation (scaled by a factor of 0.715) in the energy range $E_{\rm cm} = 3.7-6.4$ MeV. (c) Log-normal distribution fit to the ratio values shown in panel (b).

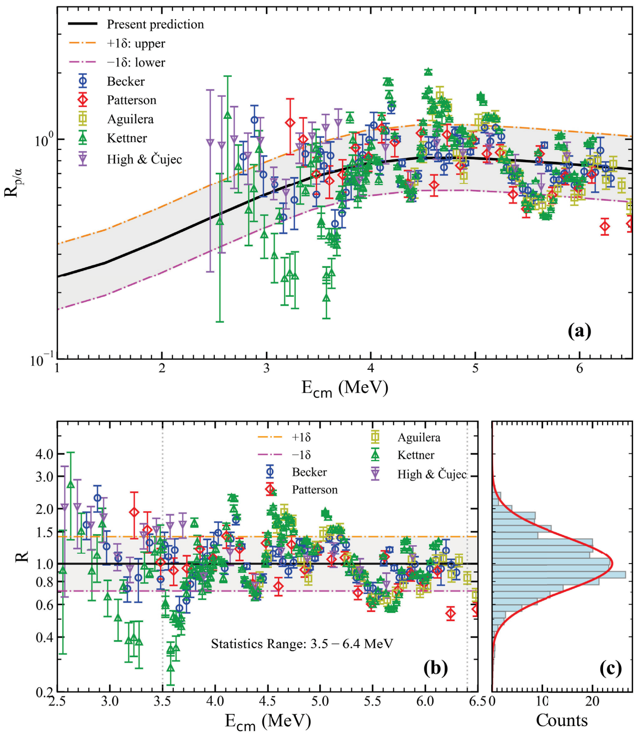

Fig. 4. (color online) (a) Experimental ratio $R_{p/\alpha}$ compared with the present prediction and its $\pm 1\delta$ uncertainty band. The comprehensive dataset includes measurements from Patterson, Becker, Aguilera, Kettner, and High and Čujec. (b) Ratio of the experimental data to the TALYS calculation (scaled by a global factor of 0.698) in the energy range $E_{\rm cm} = 3.5–6.4$ MeV. (c) Log-normal distribution fit to the ratio values shown in panel (b).

C. Comparison with indirect measurements

Deep inside the Coulomb barrier ($E_{\rm cm} < 2.5$ MeV), reliable direct measurements are extremely scarce, leaving only indirect data [21–23]. The Trojan Horse Method (THM) employed by Tumino *et al.* [23] was originally analyzed within the plane-wave approximation. While subsequent corrections using the distorted-wave approximation led to a substantially different energy dependence of the extracted cross sections, the resulting $R_{p/\alpha}$ ratio remained unaffected. Munson *et al.* [21] populated the ^{24}Mg compound nucleus through inelastic scattering of 40 MeV α particles. The resulting $R_{p/\alpha}$ ratio differs significantly from that obtained in direct measurements. This discrepancy arises because the surrogate reaction mechanism populates a spin-parity distribution that is substantially different from that produced in sub-barrier ^{12}C+^{12}C fusion. Consequently, the extracted decay branching ratios are not directly applicable to quiescent stellar carbon burning. Future indirect measurements must therefore constrain the populated spin-parity distribution in order to reliably determine the proton-to-α competition deep within the Gamow window.

In the study of $p(^{23}\text{Na},\alpha)^{20}$Ne by Nan *et al.* [22], excitation functions for the proton and α channels were measured using a thick-target inverse-kinematics approach combined with γ-particle coincidence techniques. A multi-channel R-matrix analysis revealed a series of discrete 0^+ and 2^+ resonances in the relevant energy region and provided branching ratios for the dominant decay channels across the Gamow window. These results highlight the strong energy dependence and large fluctuations of the channel competition, which have important implications for observables such as the $R_{p/\alpha}$ ratio and the resulting astrophysical reaction rates.

Figure 5 presents the combined analysis of the THM datasets reported by Tumino *et al.* [23] and Nan *et al.* [22]. As the experiments only resolved partial transitions to specific low-lying states (predominantly the p_0, p_1, α_0, and α_1 channels), the data points were corrected using the statistical-model estimates of the missing-channel branching ratios provided by Li *et al.* [7].

By applying our log-normal distribution to fit these corrected indirect datasets against the TALYS prediction within the energy range $E_{\rm cm} = 1-3$ MeV, we obtain a scaling factor of $f = 1.443$. As depicted in Fig. 5(c), the

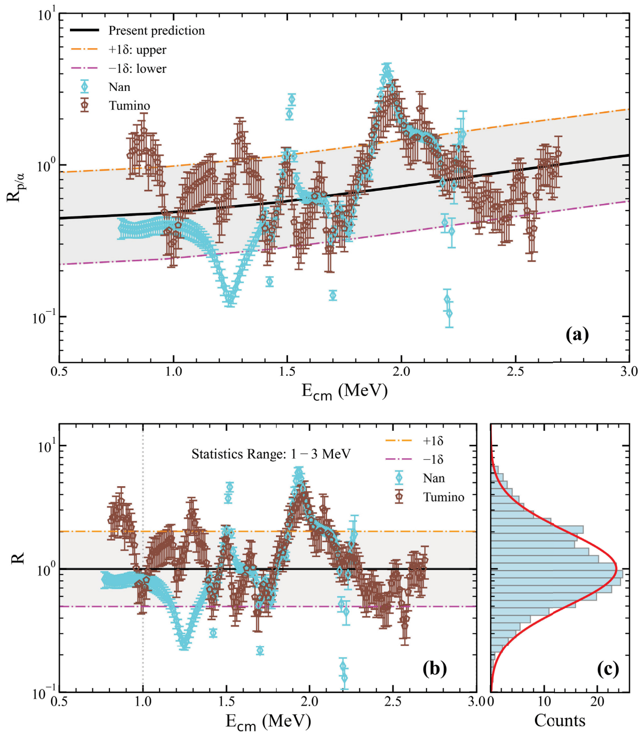

Fig. 5. (color online) (a) Experimental ratio $R_{p/\alpha}$ compared with the present prediction and its $\pm 1\delta$ uncertainty band. Data from Refs. [22, 23]. (b) Ratio of the experimental data to the TALYS calculation, which is scaled by a factor of 1.443, over the energy range $E_{\rm cm} = 1-3$ MeV. (c) Distribution of the ratio values shown in panel (b), together with a log-normal fit.

resulting log-normal distribution exhibits a broad dispersion. Most importantly, this indirectly derived scaling factor ($f = 1.443$) deviates substantially—by roughly a factor of two—from the average trend established by the direct charged-particle and gamma-ray measurements ($f = 0.698$). This striking discrepancy highlights the persistent systematic differences between direct and indirect techniques and calls for further theoretical investigation to clarify their origin.

D. Prediction of the $R_{p/\alpha}$ ratio within the Gamow window

While our predicted average $R_{p/\alpha}$ ratio is generally consistent with the CF88 [25] value (~ 0.8) above $E_{\rm cm} = 4.0$ MeV, it decreases significantly as the energy extends deeper into the Gamow window. The strong suppression of the proton channel relative to the α channel at low energies is primarily governed by the availability of decay channels.

As the center-of-mass energy decreases, the number of energetically accessible proton-emission channels diminishes much more rapidly than that of the α-emission channels. To illustrate this behavior systematically, we investigated the critical cutoff energies at which the branching ratios for specific highly excited states (*e.g.*, p_2 to p_9 and α_2 to α_5) decrease to 35% of their respective maximum values (Fig. 6). As shown in Fig. 7, at $E_{\rm cm} \sim 4.0$ MeV, where $R_{p/\alpha} \sim 0.78$, the energetically open proton-emission channels extend from p_0 to p_9, whereas the open α-emission channels are mainly limited to α_0, α_1, and α_2.

As the energy decreases further from 4.0 MeV down to 0.5 MeV, the proton-emission channels close sequentially, whereas the α_0 and α_1 channels remain open down to $E_{\rm cm} = 0$ MeV. The Q value for the $^{12}C(^{12}C, \alpha)^{20}Ne$ reaction is 4.62 MeV, substantially larger than the 2.24 MeV associated with the $^{12}C(^{12}C, p)^{23}Na$ reaction. This sequential closure of proton decay channels, originating

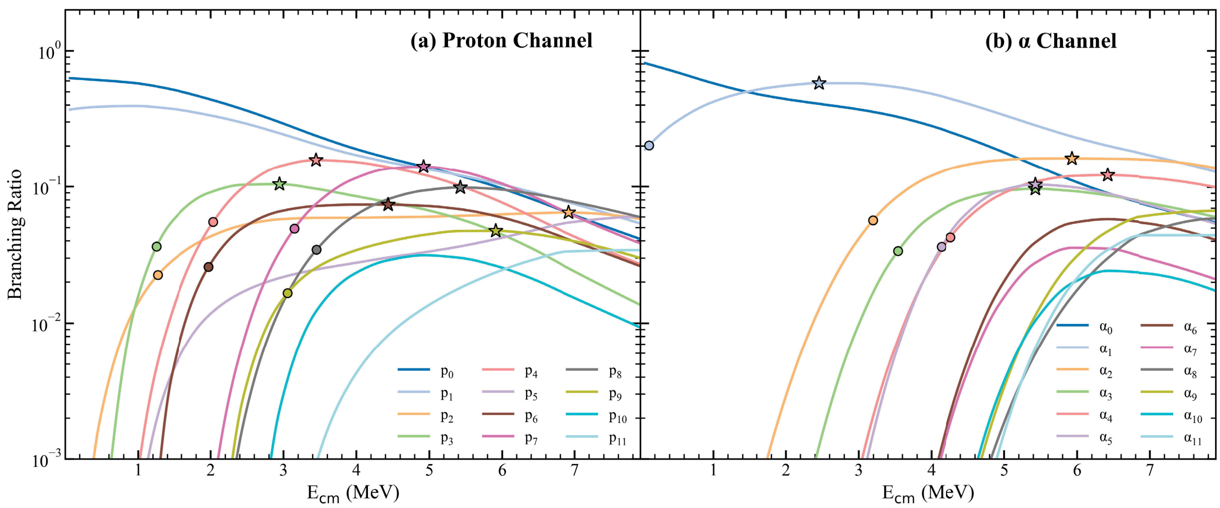

Fig. 6. (color online) The branching ratios for the different channels of $^{12}C(^{12}C,p)^{23}Na$ and $^{12}C(^{12}C,\alpha)^{20}Ne$ reactions were calculated by Li *et al.* [7]. The cut-off energies at which the branching ratio of each specific single channel (p_2, p_3, p_4, p_6, p_7, p_8, p_9, α_1, α_2, α_3, α_4, α_5) drops from its maximum value ($B_{\max}$, marked with stars) to 35% of $B_{\max}$ with decreasing energy are marked with circles.

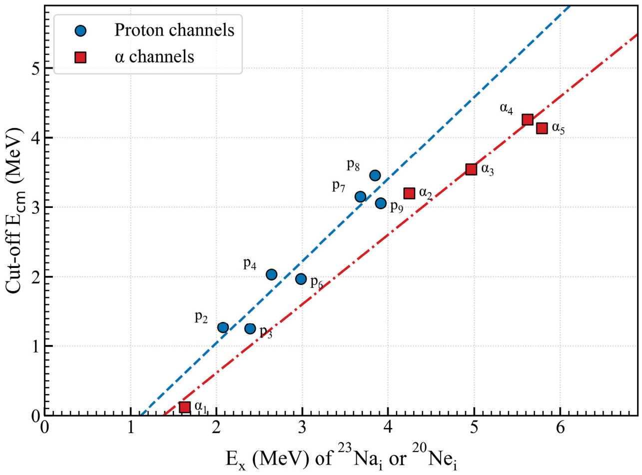

Fig. 7. (color online) The cut-off energies of specific single channels (proton: p_2, p_3, p_4, p_6, p_7, p_8, p_9; α: α_1, α_2, α_3, α_4, α_5) are plotted versus the excitation energy E_x of the corresponding ^{23}Na or ^{20}Ne nucleus. The solid circles represent the values for the proton channels (p_2, p_3, p_4, p_6, p_7, p_8, p_9); the solid squares represent the values for the α channels (α_1, α_2, α_3, α_4, α_5). These data are taken from the previous calculation by Li *et al.* [7] (Fig. 6). The dashed and dash-dotted lines are linear fits to the displayed points for the proton and α channels, respectively.

from the intrinsically smaller Q value of the proton channel, strongly suppresses the competitiveness of proton evaporation at stellar energies. Such a mechanism naturally leads to the pronounced decline of the $R_{p/\alpha}$ ratio predicted within the Gamow window.

IV. NEW REACTION-RATE RATIO, $\langle\sigma v\rangle_p/\langle\sigma v\rangle_\alpha$, AND ITS IMPACT ON ASTROPHYSICAL MODELS

We recalculated the reaction rates for ^{12}C(^{12}C,p)^{23}Na and ^{12}C(^{12}C,α)^{20}Ne by adopting the constant $S^* = 3\times10^{16}$ MeV·b recommended by CF88 for the ^{12}C+^{12}C fusion reaction, along with the $R_{p/\alpha}$ ratio established in this work. The reaction rate ratio, $\langle\sigma v\rangle_p/\langle\sigma v\rangle_\alpha$, is shown in Fig. 8. The present work reveals a pronounced temperature dependence of this ratio, which deviates significantly from the prediction of the widely used CF88 model [25].

While the CF88 compilation assumes a nearly constant $\langle\sigma v\rangle_p/\langle\sigma v\rangle_\alpha$ ratio of ~0.79 over most astrophysical temperatures, our results exhibit a strong temperature dependence. The ratio increases from 0.29 at $T_9 = 0.5$ to 0.45 at $T_9 = 1.0$, then to 0.52 at $T_9 = 1.2$, 0.70 at $T_9 = 1.8$, and ~0.78 at $T_9 = 2.5$, after which it approaches a nearly constant value. Compared with the CF88 compilation, our lower ratios at $T_9 \lesssim 1.2$ imply a stronger dominance of the α channel during hydrostatic carbon burning, potentially modifying the seed distribution for subsequent weak s-

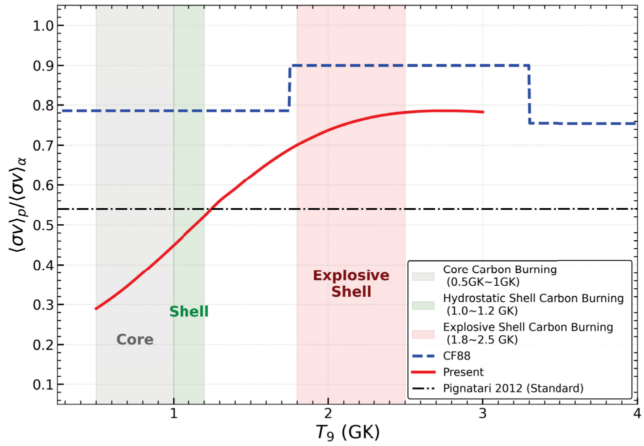

Fig. 8. (color online) Temperature dependence of the reaction rate ratio $\langle\sigma v\rangle_p/\langle\sigma v\rangle_\alpha$ from the present work (solid curve), compared with the recommended values from CF88 [25] (dashed lines) and the constant ratio of $0.35/0.65 \approx 0.54$ from Pignatari *et al.* [6] (dash-dotted line). Colored shaded regions indicate the various stages of stellar carbon burning: core carbon burning (0.5 ~ 1.0 GK, gray), hydrostatic shell carbon burning (1.0 ~ 1.2 GK, green), and explosive shell carbon burning (1.8 ~ 2.5 GK, red).

process nucleosynthesis. At explosive carbon-burning temperatures ($T_9 \gtrsim 2$), the ratio gradually approaches the CF88 prediction, indicating an increasing contribution from the proton channel in high-temperature stellar environments.

Pignatari *et al.* [6] investigated the impact of uncertainties in the carbon-burning reaction channels on stellar nucleosynthesis. They adopted three values of the reaction-rate ratio, $\langle\sigma v\rangle_p/\langle\sigma v\rangle_\alpha = 0.54$, 19, and 0.05, to explore the influence of the competition between the proton and α channels on the abundances of nuclei that serve as the primary fuel for subsequent stellar evolutionary stages. Their calculations demonstrated that the competition between the proton and α channels in the ^{12}C+^{12}C reaction plays a crucial role in determining the nucleosynthesis flow during carbon burning. In the proton-dominated scenario, proton-induced reaction chains and neutron production through the ^{13}C(α,n)^{16}O reaction are significantly enhanced, leading to stronger weak s-process nucleosynthesis and increased abundances of odd-Z nuclei such as ^{23}Na and ^{26}Al. In contrast, the strongly α-dominated scenario suppresses proton-induced reaction flows and shifts the nucleosynthesis path toward α-capture products. Our predicted average value of $\langle\sigma v\rangle_p/\langle\sigma v\rangle_\alpha$ lies much closer to the standard value of 0.54 than to either of the two extreme scenarios, as shown in Fig. 6. We suggest that incorporating these temperature-dependent ratios into stellar and galactic chemical evolution models will yield more reliable predictions of the ^{23}Na/^{20}Ne abundance ratio in massive stars.

As recently demonstrated by De Gerónimo *et al.* [2], whose calculations were based on our recommended branching ratio, uncertainties in the $\langle\sigma v\rangle_p/\langle\sigma v\rangle_\alpha$ ratio have important consequences for the structural and chemical evolution of super-asymptotic giant branch (SAGB) stars and their descendants, ultramassive white dwarfs (UMWDs). Since the proton and α channels predominantly produce ^{23}Na and ^{20}Ne, respectively, the branching ratio directly determines the chemical composition of the stellar core after carbon burning. De Gerónimo *et al.* [2] showed that the uncertainty in the branching ratio is one of the dominant sources of uncertainty in the final chemical structure of SAGB progenitors. In particular, a stronger α channel (corresponding to a lower $\langle\sigma v\rangle_p/\langle\sigma v\rangle_\alpha$ ratio) substantially enhances the central ^{20}Ne abundance, with variations reaching up to ~17%. Such changes in the ^{20}Ne/^{16}O ratio affect the crystallization, cooling behavior, and pulsational properties of the resulting UMWDs.

The branching ratio also influences the threshold mass for carbon ignition. Because the α channel releases more energy than the proton channel, a stronger α channel increases the efficiency of carbon burning and allows carbon ignition to occur at slightly lower stellar masses. De Gerónimo *et al.* [2] found that the minimum zero-age main-sequence (ZAMS) mass required to experience a carbon flash may decrease by approximately 1.5% when the α channel dominates. In addition, the mass range in which carbon burning remains partially incomplete is sensitive to the adopted $\langle\sigma v\rangle_p/\langle\sigma v\rangle_\alpha$ ratio.

We acknowledge that extrapolating the Hauser-Feshbach statistical model into the deep sub-Coulomb Gamow window ($E_{\rm cm} < 3$ MeV) encounters inherent physical limitations. In this regime, the level density of the compound nucleus ^{24}Mg is relatively low, and the reaction mechanism is strongly modulated by discrete, structured molecular resonances rather than overlapping statistical states. Our physically calibrated TALYS prediction serves as an average statistical trend. In stellar environments, the reaction rate is an integral over the Gamow window. While individual discrete resonances will undoubtedly cause local fluctuations in the $R_{p/\alpha}$ ratio, their energy-averaged collective behavior is expected to follow this statistical trend. Most importantly, providing an energy-dependent, theoretically and experimentally constrained average trend of $\langle\sigma v\rangle_p/\langle\sigma v\rangle_\alpha$ represents a significant improvement over the arbitrary constant branching ratio historically adopted in standard astrophysical networks (*e.g.*, CF88) and provides a more realistic "prior" for future R-matrix evaluations of specific discrete resonances.

V. SUMMARY

In summary, we have investigated the energy dependence of the ^{12}C(^{12}C$,p$)^{23}Na to ^{12}C(^{12}C$,\alpha$)^{20}Ne branching ratio and its impact on carbon-burning nucleosynthesis. A careful re-examination of sub-barrier experimental data reveals significant discrepancies at $E_{\rm cm} < 3.0$ MeV. By focusing on the more consistent high-energy regime, we derived a new temperature-dependent branching ratio for astrophysical environments. Our results demonstrate that $R_{p/\alpha}$ is not a constant but evolves dynamically with temperature, and $\langle\sigma v\rangle_p/\langle\sigma v\rangle_\alpha$ decreases from approximately 0.78 at $T_9 = 2.5$ to 0.29 at $T_9 = 0.5$.

The deviation from the traditional CF88 constant ratio may have implications for the various stages of hydrostatic carbon burning and the subsequent formation of white dwarfs. While the present statistical framework cannot fully resolve the structures of isolated resonances, the temperature-dependent $\langle\sigma v\rangle_p/\langle\sigma v\rangle_\alpha$ averaged trend established in this work provides a physically motivated alternative to the widely adopted CF88 constant values. This energy-dependent trend serves as an updated reference for modeling stellar chemical evolution. Ultimately, determining the exact branching ratios still awaits high-precision direct measurements deep within the Gamow window.

References

[1] L. R. Gasques, A. V. Afanasjev, E. F. Aguilera *et al*, Phys. Rev. C **72**(2), 025806 (2005)

[2] F. C. De Gerónimo, M. M. Miller Bertolami, T. Battich *et al*, Astrophys. J. **975**(2), 259 (2024)

[3] A. Chieffi, S. Courtin, R. J. Deboer *et al*, Eur. Phys. J. A **61**(12), 280 (2025)

[4] M. Wiescher, C. A. Bertulani, C. R. Brune *et al*, Rev. Mod. Phys. **97**(2), 025003 (2025)

[5] J. R. Patterson, H. Winkler, C. S. Zaidins, Astrophys. J. **157**, 367 (1969)

[6] M. Pignatari, R. Hirschi, M. Wiescher *et al*, Astrophys. J. **762**(1), 31 (2012)

[7] Y. J. Li, X. Fang, B. Bucher *et al*, Chin. Phys. C **44**(11), 115001 (2020)

[8] A. J. Koning, S. Hilaire, M. C. Duijvestijn, AIP Conf. Proc. **769**, 1154 (2005)

[9] A. Koning, S. Hilaire, S. Goriely, Eur. Phys. J. A **59**(6), 1 (2023)

[10] W. Hauser, H. Feshbach, Phys. Rev. **87**(2), 366 (1952)

[11] K. Hagino, N. Rowley, A. T. Kruppa, Comput. Phys. Commun. **123**, 143 (1999)

[12] M. G. Mazarakis, W. E. Stephens, Phys. Rev. C **7**(4), 1280 (1973)

[13] M. D. High, B. Čujec, Nucl. Phys. A **282**(1), 181 (1977)

[14] K. U. Kettner, H. Lorenz-Wirzba, C. Rolfs *et al*, Phys. Rev. Lett. **38**(7), 337 (1977)

[15] K. U. Kettner, H. Lorenz-Wirzba, C. Rolfs, Z. Phys. A **298**(1), 65 (1980)

[16] H.-W. Becker, K. U. Kettner, C. Rolfs *et al*, Z. Phys. A **303**(4), 305 (1981)

[17] E. F. Aguilera, P. Rosales, E. Martinez-Quiroz *et al*, Phys. Rev. C **73**(6), 064601 (2006)
[18] L. Barrón-Palos, E. F. Aguilera, J. Aspiazu *et al*, Nucl. Phys. A **779**, 318 (2006)
[19] T. Spillane, F. Raiola, C. Rolfs *et al*, Phys. Rev. Lett. **98**, 122501 (2007)
[20] G. Fruet, S. Courtin, M. Heine *et al*, Phys. Rev. Lett. **124**(19), 192701 (2020)
[21] J. M. Munson, E. B. Norman, J. T. Burke *et al*, Phys. Rev. C **95**(1), 015805 (2017)
[22] W. Nan, Y. Wang, J. Su *et al*, Phys. Lett. B **862**, 139341 (2025)
[23] A. Tumino, C. Spitaleri, M. La Cognata *et al*, Nature **557**(7707), 687 (2018)
[24] K. A. Li, Y. H. Lam, C. Qi *et al*, Phys. Rev. C **94**(6), 065807 (2016)
[25] G. R. Caughlan, W. A. Fowler, At. Data Nucl. Data Tables **40**(2), 283 (1988)